Enhancing Through Air Drying Process Efficiency: Investigating Laboratory-to-Pilot Scale Correspondence and Impact of Process Variables on Tissue Paper Manufacturing

Björn Sjöstrand,[a,*] Bruno Tremblay,[b] and Mikael Danielsson [c]

State-of-the-art manufacturing of tissue paper by Through Air Drying provides excellent product performance, although at a high production cost and energy use. In this work, a laboratory scale vacuum suction box was used to mimic the initial dewatering and the Through Air Drying molding, together with a pilot-scale trial. The purpose was to investigate both how the laboratory scale corresponds to pilot scale testing and investigate how fabric design, basis weight, beating, and fibers affect dewatering and sheet caliper. This study reevaluates dewatering mechanisms during molding, challenging the previous hypothesis of pure air displacement dewatering. Results show a parallel mechanism of compression dewatering and air displacement. The influence of rush transfer is examined, impacting the sheets' visual appearance, thickness, and solids content. Correlations between molding box solids content and headbox freeness emphasize significance of fibers and beating levels. Pilot results confirm the link between former solids and molding box solids. Pilot trials validate the laboratory results, facilitating comprehensive simulation of full-scale manufacturing. This research reveals dewatering mechanisms, highlights operational parameters, and enables effective Through Air Drying process design and refinement.

DOI: 10.15376/biores.18.4.8264-8283

Keywords: Through air drying; TAD; Dewatering; Vacuum dewatering; Molding; Energy efficiency; Tissue

Contact information: a: Pro2BE, the Research Environment for Processes and Products for a Circular Forest-based Bioeconomy, Department of Engineering and Chemical Sciences, Karlstad University, Sweden; b: Concept Manager, TAD Technology, Valmet AB, Sweden; c: Polyniora, Halmstad, Sweden.
**Corresponding author: bjorn.sjostrand@kau.se*

INTRODUCTION

The global tissue market has witnessed significant growth, which can be attributed to rising demand for quality hygiene products that enhance the quality of life. The market offers a variety of tissue paper products, such as paper towels, napkins, facial tissues, and toilet paper, that have become integral to modern living. These products contribute significantly to improving hygiene standards, providing comfort and convenience, and limiting the spread of disease (Vieira *et al.* 2023). Currently, with increasing demands on sustainability, efficient management of energy use, raw materials, machine clothing, and wet end chemicals are crucial for the success of tissue making. Although mills can generate around 50% of their required energy using biomass residues, this is rarely the case in tissue production. Therefore, there is a significant potential for improving the energy efficiency

of tissue-making processes (Håkansson 2010; Lahtinen and Karvinen 2010; Holmberg *et al.* 2013; Sjöstrand 2020).

A Through Air Drying (TAD) machine (Fig. 1) differs from a conventional dry creped tissue (DCT) machine, where the press is replaced by one or two TAD cylinders, and a structured molding TAD fabric receives the sheet by transfer with vacuum boxes. Water is removed before and during TAD molding (Sjöstrand *et al.* 2023) and also by hot air blown through the perforated TAD cylinders. The tissue sheet's structure and bulk are primarily attributed to the structured TAD fabric. There is a noticeable speed difference between the forming section and TAD section, which significantly influences sheet properties compared to DCT by providing an effect related to creping. Although the lack of wet pressing in the TAD method makes it less energy efficient than DCT, TAD yields higher performing products compared to DCT (Tysén 2018; Sjöstrand *et al.* 2023).

Fiber blends consisting of a mixture of softwood and hardwood are primarily used in the production of tissue papers (de Assis *et al.* 2018). The wood species have different fiber types with varying dimensions, and this can affect drainage and dewatering, also by their varying fines content (de Assis *et al.* 2018). Fines will give a negative effect on drainage by blockage of drainage channels (de Assis *et al.* 2018; Hubbe *et al.* 2020). For wood species with flexible fibers, the conformability of each fiber can impact dewatering by causing the surface of the forming fabric to seal (Sjöstrand *et al.* 2019; Hubbe *et al.* 2020).

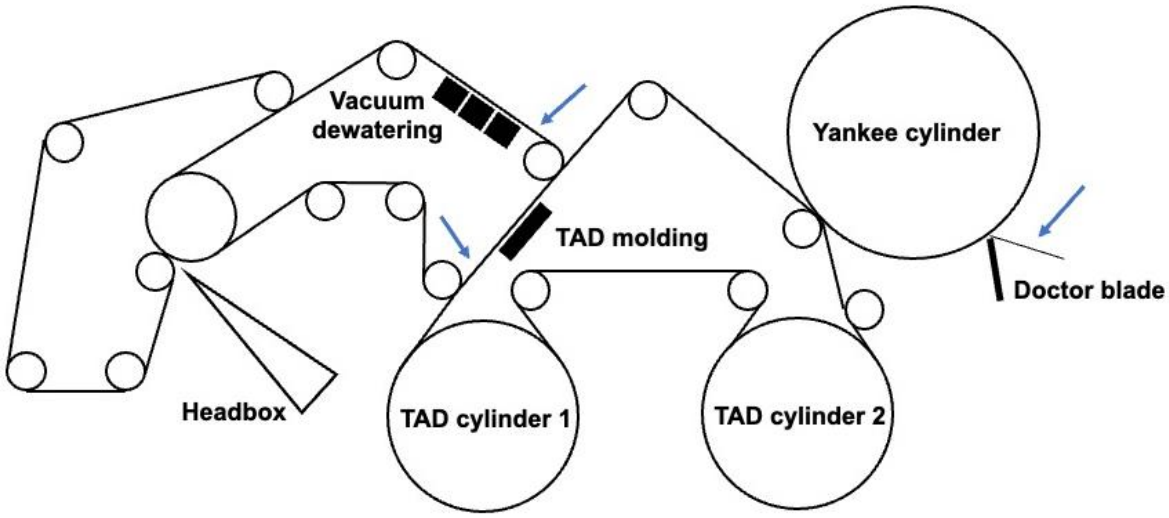

Fig. 1. Setup of the TAD tissue machine in pilot scale used during the trials. The headbox distributes the fibers between two forming fabrics. The sheet is dewatered with several suction boxes. After vacuum dewatering, the sheet is molded into the TAD fabric by vacuum. In the TAD cylinders the sheet is subjected to flow of air through the structure, drying the sheet, followed by conventional Yankee drying with creping. Blue arrows indicate measurement locations for solids content evaluation, before and after molding and after Yankee drying.

Previous research (Ramaswamy 2003; Pujara *et al.* 2008) established that the dewatering performance of vacuum suction boxes aligns with the general dewatering pattern observed in paper production. Specifically, the initial stage involves easy removal of water, while the later stages involve more challenging water extraction, resulting in diminishing returns (Attwood 1962; Neun 1994, 1996; Räisänen *et al.* 1996; Ramaswamy 2003; Pujara *et al.* 2008). The progressively challenging dewatering process is attributed to the positioning of water within the sheet's structure. The elimination of water occurs

sequentially, starting with the extraction of water from the spaces between the fibers, followed by the removal of water from the lumen, and ultimately, from the fiber walls (Paulapuro 2000; Stenström and Nilsson 2015). Various factors, including sheet basis weight, forming fabric, pulp beating, vacuum level, and dwell time, have been demonstrated to impact vacuum dewatering. Additionally, it has been established that drainage is the primary dewatering mechanism that occurs before vacuum dewatering takes place (Britt and Unbehend 1985), compression dewatering happens initially during vacuum exposure (Åslund and Vomhoff 2008a,b), followed by air displacement dewatering when air channels appear (Räisänen *et al.* 1996; Åslund and Vomhoff 2008b; Nilsson 2014a,b), and finally external rewetting after vacuum exposure (Åslund *et al.* 2008b; Sjöstrand *et al.* 2015).

Tysén *et al.* (2015, 2018) published a lot of work related to TAD tissue manufacturing. They explained the effects of basis weight and pulp type on water removal with TAD at a laboratory scale (Tysén *et al.* 2015) and investigated the effects on TAD dewatering assisted with infrared radiation (Tysén *et al.* 2018). The proposed mechanism for dewatering involved the evaporation process facilitated by air flow, with an additional increase in drying capacity of the TAD attributed to an elevation in temperature resulting from infrared radiation. However, the relatively long dwell times employed in the experiment make it challenging to establish a direct correlation between the results obtained and those expected in pilot and full-scale tissue production processes (Tysén *et al.* 2015, 2018).

Previously, a laboratory method for measuring the initial vacuum dewatering on the forming fabric, as well as the dewatering during TAD molding was developed (Sjöstrand *et al.* 2023). The developed method were used in this work to investigate the influence of different TAD fabric designs, sheet basis weights, pulp beating level, and fiber mixtures, on the dewatering and energy efficiency during vacuum dewatering and TAD molding. The laboratory results were also validated by pilot scale measurements of selected settings of pulp types, basis weight, beating levels, and fabric designs.

EXPERIMENTAL

Fibers and Fabrics

Bleached unbeaten chemical kraft hardwood pulp fibers from eucalyptus and softwood pulp fibers from a mix of spruce and pine were supplied by Valmet AB (Karlstad, Sweden) for the laboratory trials, with a solids content of approximately 95%. The same fiber types were used for the pilot trial. Both pulps were characterized with a Valmet Fiber Image Analyzer (Valmet FS5, Valmet AB, Karlstad, Sweden). The fiber length was approximately 0.8 mm and the fiber width was 13 μm for the hardwood fibers, and 1.9 mm and 24 μm for the softwood fibers, based on single tests in the FS5. The drainage resistance was measured with the Shopper-Riegler method, ISO 5267-1 (1999) to a value of 15.5 °SR for hardwood and 13.5°SR for softwood fibers. To be able to test beaten fibers in laboratory scale, additional never-dried bleached beaten chemical kraft softwood pulp fibers mixed from spruce and pine were supplied by StoraEnso AB (Skoghall, Sweden) with a solids content of 4%. The never-dried softwood pulp was characterized with an L&W Fiber Tester (ABB AB / Lorentzen and Wettre, Kista, Sweden). The fiber length was 2.2 mm, and the fiber width was 31 μm based on a single test in the fiber tester. The drainage

resistance was measured with the Shopper-Riegler method, ISO 5267-1 (1999) to a value of 23 °SR. For both FS5 and fiber tester the single values of fiber length were based on many images of individual fibers in the pulp samples.

The furnish used for the pilot machine trial was mixed from the same fiber types as the laboratory trials, spruce and pine mix and eucalyptus according to the description above. Wet-end chemicals for towel grade production, such as wet-strength resin and an anionic cofactor dry-strength additive, were used and kept constant during the test.

The TAD configuration used requires three fabrics. Thus, there were two forming fabrics (inner and outer forming fabric) and a TAD or molding fabric. The basic fabric data are presented in Table 1. The outer forming fabric is a thin triple layer fabric with high dewatering capacity, whereas the inner forming fabric is a triple layer fabric made to ensure good dewatering balanced with safe pick up at the forming position and a safe transfer over to the TAD fabric. The TAD fabric is a relatively coarse single layer fabric mainly used for towel tissue applications. The TAD fabrics evaluated were based on the same design, an eight shed single layer fabric, see Fig. 2, where the yarns and yarn density, both in machine direction (MD) and cross machine direction (CD). These were varied to generate different fabric properties, such as fabric caliper, thickness, and openness, measured as air permeability. These fabric properties have a significant influence on sheet characteristics, and the intention in this work was to investigate how varying fabric properties relate to or would affect the dewatering performance. The designs are mainly used for towel tissue applications. The fabrics were provided by Albany International Inc. (Rochester, NH, USA).

Table 1. Yarn Set Up in Machine and Cross Machine Direction for the Forming Fabrics, MD, and CD, and Basic Data for Caliper and Permeability

	Yarn Density		**Yarn Diameter**		**Caliper**	**Air Perm.***
	MD	CD	MD	CD		
	(Yarns/cm)	(Yarns/cm)	(mm)	(mm)	(mm)	(cfm)
Forming fabrics						
Inner	75	54/10**	0.15	0.13/0.20**	0.645	380
Outer	76	36/18**	0.125	0.13/0.20**	0.610	517

* ASTM D737-96 (2017)
**Fine/coarse

Table 2. Yarn Set Up in Machine and Cross Machine Direction for the TAD Fabrics, MD and CD, and Basic Data for Caliper and Permeability

	Yarn Density		**Yarn Diameter**		**Caliper**	**Air Perm.***
	MD	CD	MD	CD		
	(Yarns/cm)	(Yarns/cm)	(mm)	(mm)	(mm)	(cfm)
TAD fabrics						
1	18.4	11.0	0.35	0.45	1.20	710
2	18.0	11.2	0.35	0.50	1.15	625
3	17.9	10.3	0.35	0.55	1.20	600
4	17.8	9.6	0.35	0.60	1.27	600
5	15.7	10.6	0.40	0.55	1.29	600

* ASTM D737-96 (2017)
**Fine/coarse

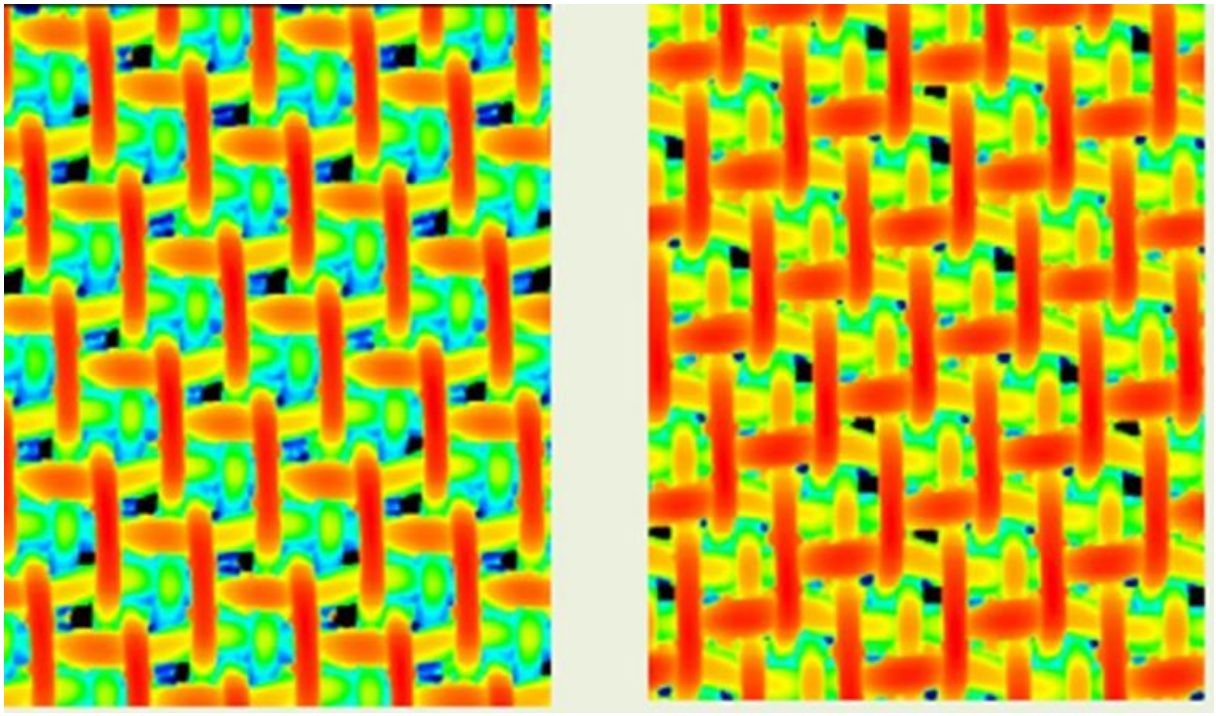

A B

Fig. 2. Topographic images from the basic TAD fabric design used, paper side (A) and back side or wear side (B)

Laboratory Trial

The trial setup had several parameters varied, such as sheet basis weight, fiber mixtures, fiber beating level, and TAD fabric design. The fabrics used were the inner fabric from Table 1 and the five variations of TAD fabrics from Table 2. The trial setup is summarized in Table 3. Only one parameter was varied at once, and the bold variations in Table 3, were the default settings.

Table 3. Trial Setup

Parameter	Variations
Basis weight	**20**, 25, 30 g/m^2
Fiber mixture	**75/25**, 60/40, 90/10 (SW/HW)
Fiber beating level	Unbeaten, **Beaten**
TAD fabric design	**1**, 2, 3, 4, 5

Bold variations were set at the standard parameters and kept constant when the others were varied

All variations from Table 3 were subjected to vacuum dewatering and TAD molding in laboratory scale according to the new method developed in a previous article by Sjöstrand *et al.* (2023). All testing were carried out in room temperature of approximately 20 °C and without controlled humidity. Fiber mixtures were diluted to 0.2% in tap water with no wet end chemicals added. These stock solutions were assumed to have densities of 1 g/cm^3; this assumption is believed to be valid because the fibers are a small part of the total weight and also totally saturated with water. The appropriate amount of stock solution, regulated by desired basis weight, was measured on a scale and added to a modified sheet former together with an additional approximately 3.5 L of tap water. The

sheet former had a diameter of 18.4 cm, and the sheet was formed directly on the commercial inner forming fabric described above. The tissue sheet that had been formed on the forming fabric had a solids content of around 6%. The sheet was moved from the sheet former, still on the fabric, to the vacuum dewatering equipment (Fig. 3), which was described in detail by Granevald *et al.* (2004) with a plate mounted with a single 5 mm opening. The tissue paper and the forming fabric, was then exposed to a pressure drop of -30 kPa for different dwell times (0, 1, 2.5, 5, 10, and 20 ms) in triplets, to simulate dewatering in a typical suction box. To measure solids content, each tissue sheet was scraped off the forming fabric before and after each vacuum dewatering run, and a solids content measurement was taken on the 10 cm diameter middle part of the sheet using the ISO 638-1 (2022) standard. Because the edges of the sheets were not completely dewatered, only the middle part was used for measurements. All solids content measurements were taken after complete rewetting, as it was found by Sjöstrand *et al.* (2015) that rewetting occurred in less than 1 s.

Additionally, tissue sheets already dewatered 20 ms on the forming fabric were manually transferred to the TAD fabric and brought back to the vacuum suction box, with no speed differential between fabrics. The machine exposed these sheets a second time with -65 kPa to mimic the TAD molding, using the following dwell times: 2.5, 5, 10, and 20 ms. After TAD dewatering, these tissue sheets were evaluated for solids content according to ISO 638-1 (2022). The sheets will be subjected briefly to air drying, during the approximately 30 s, between the first and the second run. The effects of this are believed to be minimal and equal for all samples, thus they were neglected for this study.

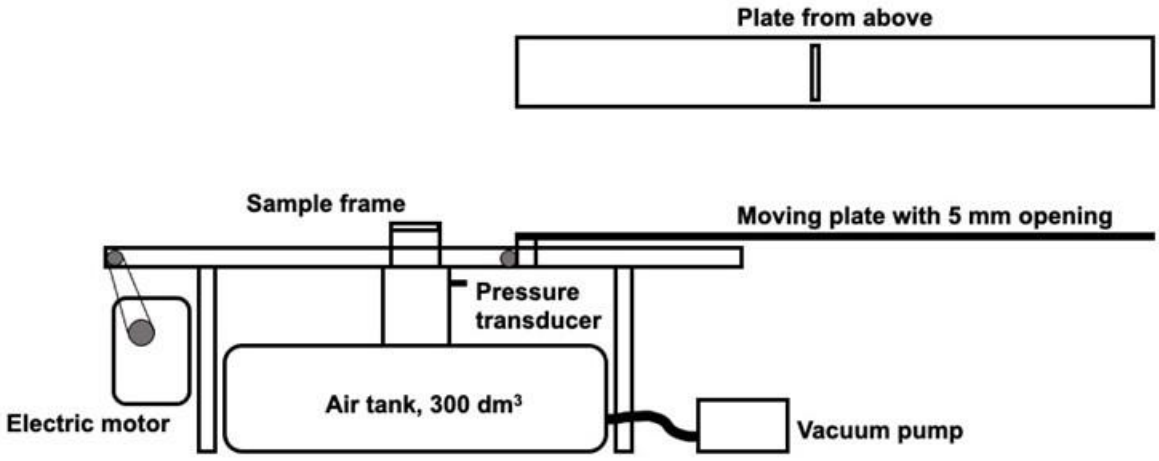

Fig. 3. Schematic drawing of the custom-built laboratory scale vacuum suction box. The pressure drop is varied with the vacuum pump and measured with the pressure transducer. The vacuum dwell time is varied with varying speeds of the moving plate, dwell time can be as small as 0.5 ms. The sheet is supported in the sample frame by either forming fabrics or TAD fabrics.

The pressure was measured continuously during the sampling in the vacuum dewatering machine, both for forming fabric dewatering and TAD dewatering. The logged pressure drops of each sheet's exposure of vacuum dewatering were used to calculate the air volume that passed through the sheet using Eq. 1 (Granevald *et al.* 2004; Sjöstrand *et al.* 2016). The air volume for TAD sheets shown in the results were the addition of both the forming fabric dewatering air volume for 20 ms, and the corresponding TAD

dewatering air volume, because these sheets effectively are dewatered twice, one time supported by the forming fabric and then again supported by the TAD fabric. The penetrated air volume (dm^3) is given by Eq. 1, as follows,

$$V_{\text{air}} = \frac{V_{\text{tank}}}{P_{\text{atm}}} \times \Delta P \quad (1)$$

where V_{tank} is the volume of the tank (dm^3), P_{atm} is the atmospheric pressure (Pa), and ΔP is the change in pressure during the test (Pa), as explained by Granevald *et al.* (2004).

The TAD dewatered laboratory handsheets were dried at room temperature, without prior pressing or drying restraints, to conserve the structure.

Pilot Trial

A pilot trial was conducted at the Valmet Tissue Technology Center in Karlstad Sweden. The machine configured to the TAD process. The forming and TAD fabrics were the same as in the laboratory trials. Thus, the inner and outer forming fabric were according to Table 1 and TAD fabric design 2 in Table 2. This TAD fabric is a standard TAD towel fabric. Process variables, such as basis weight, refining level, and furnish, were varied. The pilot trial is summarized in Table 4. A turnover time of 15 min, combined with allowing the machine to stabilize for an additional 15 min, insured a residence time greater than 30 min prior to sampling. Other machine parameters remained constant. For the duration of the trial, the rush transfer was adjusted at 12%, while the reel crepe was set at 0%. These are normal levels for TAD towel production. Because time was limited, drying was adjusted for maintaining an acceptable machine operation. Therefore, the final solids content of the paper did not always exactly reach the target.

Solids content samples were collected after each dewatering element by blowing the sheet off the fabric (at constant air pressure). A total of three samples was collected for each dewatering element and condition. An average solids content value was then calculated from the three samples along with 95% confidence intervals.

Table 4. Setup for the Pilot Machine Trial with Ten Different Machine Settings*

Test	Reel Basis Weight (Bone Dry) g/m²	Wet-end Basis Weight (g/m²)	Softwood (%)	Hardwood (%)	SW Refining (kWh/MT)
0	22.4	20	75	25	50
1	22.4	20	75	25	50
2	22.4	20	75	25	120
3	22.4	20	75	25	15
4	22.4	20	50	50	15
5	22.4	20	50	50	120
6	22.4	20	100	0	15
7	22.4	20	100	0	120
8	29.1	26	75	25	50
9	17.5	15.6	75	25	50
10	17.5	15.6	75	25	50

*Corresponding to the laboratory test series within the limits of what is possible on the pilot scale TAD machine; Test 0 is identical to Test 1 without rush transfer

Sheet Characterization

All laboratory and pilot machine sheets were characterized for one of the most important properties of kitchen towel tissue sheets, sheet caliper, by measuring single ply thickness according to ISO 12625-3 (2014) on conditioned sheets according to ISO 187 (2022). The sheet caliper was measured on a single sheet, repeated ten times to enable calculation of standard deviation and 95% confidence interval. The sheets' appearance was also qualitatively captured with scanning electron microscopy (SEM) with a Hitachi SU-3500 (Tokyo, Japan) instrument. The SEM was an environmental SEM with normal conditions and no metal plating of the material.

Note that for pilot test 3, the conditions made it unable to make a paper roll due to low paper strength and paper testing was not performed, all dryness tests were however successful for all pilot tests, including Test 3.

RESULTS AND DISCUSSION

Sheet Characterization

The sheet caliper for each sheet for different settings are shown in Tables 3 through 7. The results are quite expected, where only minor differences in single ply thickness can be observed for the TAD fabrics (Tables 3 and 4). This was despite the fact that thickness measured on multiple plies might have either additive effects of the structural embossing made by the fabrics, or there might be different packing behavior where the deformations fit each other and become less apparent. For the increasing basis weights in Table 5, the sheet thickness increased with increasing basis weight, which was expected. The beating levels, Table 6 and 7, also followed the expected pattern where less beating gave less collapsed fibers, and thus a bulkier structure and higher thickness. Note that the hardwood fibers were unbeaten, which is the reason for the 60/40 SW/HW mix to have higher thickness with the same argumentation as the unbeaten softwood fibers. Table 9 shows caliper (mm) of pilot TAD sheets that are generally larger than the laboratory sheets. This is explained by the much more efficient rush transfer and TAD molding into the structure of the TAD fabric on a moving pilot machine relative the stationary laboratory suction box with sheet transfer between fabrics by hand. A closer look at difference in thickness between Test 0 and Test 1 show this, because the 0.02 mm difference between the two is solely attributable to the rush transfer, which is the only difference between the two tests.

Table 5. Single Ply Thickness (mm) for TAD Fabrics 1-5

Sample	Single Ply Thickness (mm)
TAD1 75/25 mix, 20 g/m^2, beaten	0.11 ± 0.003
TAD2 75/25 mix, 20 g/m^2, beaten	0.12 ± 0.006
TAD3 75/25 mix, 20 g/m^2, beaten	0.12 ± 0.003
TAD4 75/25 mix, 20 g/m^2, beaten	0.11 ± 0.003
TAD5 75/25 mix, 20 g/m^2, beaten	0.11 ± 0.002

All samples had a 75/25 SW/HW mix, beaten softwood pulp, and 20 g/m^2 sheets; Variance is shown as 95% confidence interval based on ten repetitions.

Table 6. Single Ply Thickness (mm) for TAD Fabric 1, 75/25 SW/HW Fiber Mix, 20, 25, and 30 g/m^2

Sample	Single Ply Thickness (mm)
TAD1 75/25mix, 20 g/m^2, beaten	0.11 ± 0.003
TAD1 75/25mix, 25 g/m^2, beaten	0.15 ± 0.004
TAD1 75/25mix, 30 g/m^2, beaten	0.17 ± 0.009

Variance is shown as 95% confidence interval based on ten repetitions.

Table 7. Single Ply Thickness (mm) for TAD Fabric 1, 20 g/m^2, Beaten Fibers with 60/40, 75/25, and 90/10 SW/HW fiber Mixtures

Sample	Single Ply Thickness (mm)
TAD1 75/25 mix, 20 g/m^2, Beaten	0.11 ± 0.003
TAD1 60/40 mix, 20 g/m^2, Beaten	0.12 ± 0.004
TAD1 90/10 mix, 20 g/m^2, Beaten	0.11 ± 0.004

Variance is shown as 95% confidence interval based on ten repetitions.

Table 8. Single Ply Thickness (mm) for Unbeaten and Beaten Softwood Fibers Using TAD Fabric 1, 75/25 SW/HW Fiber Mix, Sheets of 20 g/m^2

Sample	Single Ply Thickness (mm)
TAD1 75/25 mix, 20 g/m^2, beaten	0.11 ± 0.003
TAD1 75/25 mix, 20 g/m^2, unbeaten	0.13 ± 0.005

Variance is shown as 95% confidence interval based on ten repetitions.

Table 9. Single Ply Thickness (mm) of Pilot Sheets, machine settings, fiber mix and beating levels shown in Table 4

Test	Single Ply Thickness (mm)
0	0.13 ± 0.004
1	0.15 ± 0.007
2	0.16 ± 0.002
3	**No paper on reel**
4	0.15 ± 0.004
5	0.14 ± 0.003
6	0.14 ± 0.004
7	0.14 ± 0.005
8	0.17 ± 0.004
9	0.12 ± 0.002
10	0.13 ± 0.003

Variance is shown as 95% confidence interval based on five repetitions; for test 3, no paper was on the reel due to low sheet strength.

Laboratory Trial

The dewatering behavior during both forming fabric (FF) vacuum dewatering and TAD molding is shown for all samples in Figs. 4 through 7, along with the corresponding volumes of penetrated air during testing. The air volumes are directly connected to the pump energy in the vacuum section and thus connected to energy consumption of the

process (Sjöstrand 2023). The dewatering behavior for the forming fabric was expected and in line with previous observations of vacuum dewatering and penetrated air volume (Attwood 1962; Neun 1994, 1996; Räisänen *et al.* 1996; Ramaswamy 2003; Pujara *et al.* 2008; Sjöstrand *et al.* 2016, 2017, 2019; Rahman *et al.* 2018; Sjöstrand and Brolinson 2022; Sjöstrand *et al.* 2023; Sjöstrand 2023).

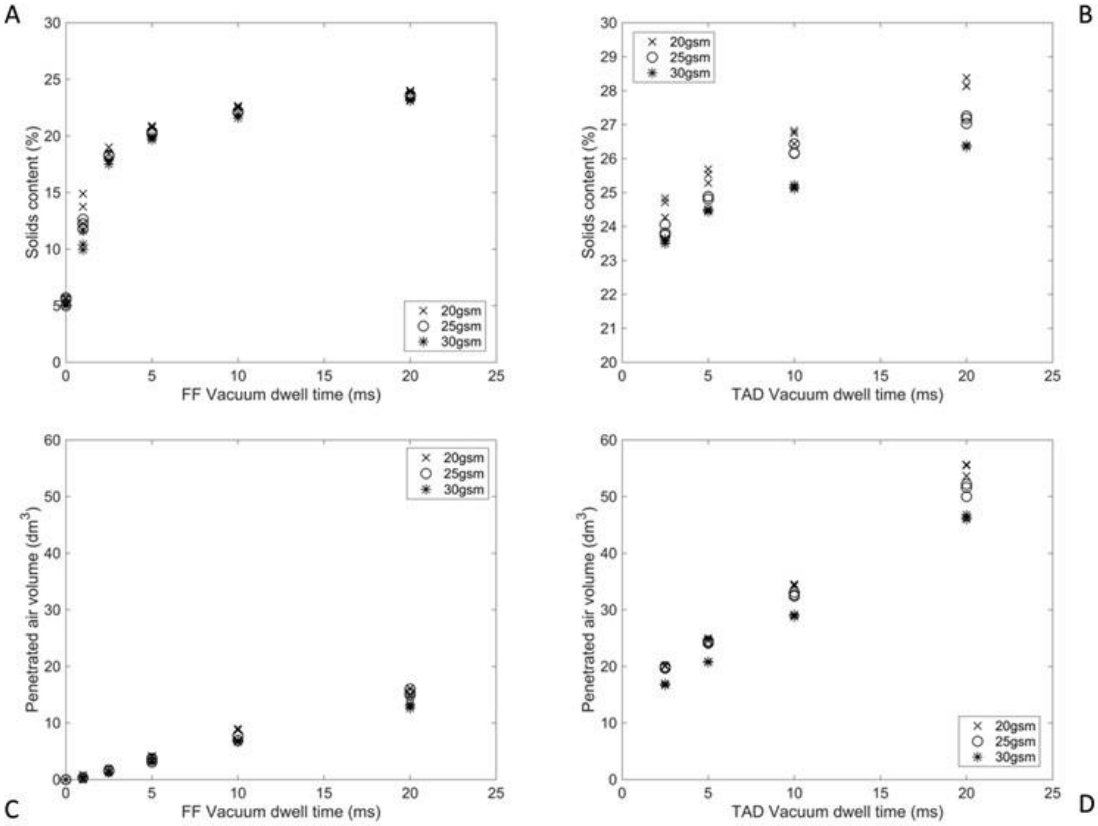

Fig. 4. Solids content (%) *versus* vacuum dwell time (ms) on the forming fabric (FF) (A), TAD fabric 1 (B) and penetrated air volume (dm^3) on the forming fabric (C), and TAD fabric 1 (D) in laboratory trials for three different basis weights. The fiber mix was 75/25 SW/HW and sheet basis weight 20 g/m^2.

According to the laboratory results of solids content development for TAD fabrics (Fig. 4B), the solids increased with a similar shape of diminishing returns, for the different forming fabrics (Fig. 4A). This contradicts the hypothesis presented in Sjöstrand *et al.* (2023), where the mechanism of TAD dewatering was proposed to consist mainly of air displacement dewatering. The results from different sheet basis weights (Fig. 4B) suggest that there might be enough water still present in the structure for a combination of compression dewatering and air displacement dewatering. The same behavior can be observed for different fiber mixes (Fig. 5B) and for different beating levels (Fig. 6B).

The forming fabric dewatering and the penetrated air volume development for both forming fabrics and TAD fabrics (Figs. 4 through 7) show expected behaviors, with linear increase in air volume and diminishing returns for forming fabric dewatering. The penetrated air volumes of TAD dewatering indicate that the process requires huge amounts of pumping energy.

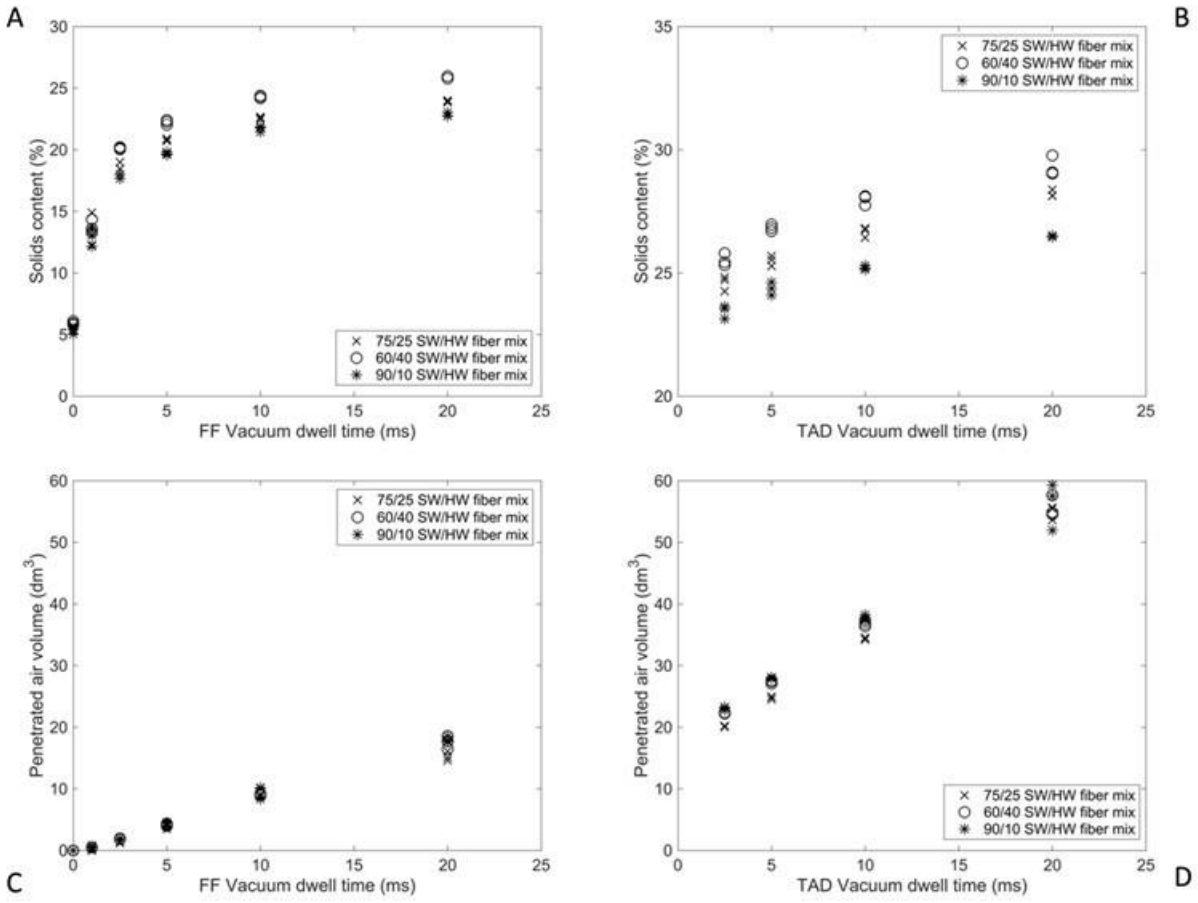

Fig. 5. Solids content (%) *versus* vacuum dwell time (ms) on the forming fabric (FF) (A), TAD fabric 1 (B) and penetrated air volume (dm^3) on the forming fabric (C), and TAD fabric 1 (D) in laboratory trials for three different fiber mixes, sheet basis weight 20 g/m^2

Figures 6 and 7 reveal that significant differences in solids leaving both forming section and molding can be achieved with small differences in penetrated air volume, which in turn is connected to energy expended. The two beating levels in Fig 6A and 6B show much higher solids contents for the unbeaten SW pulp compared to the beaten pulp, although the differences in penetrated air volumes in Fig. 6C and 6D are relatively unchanged. For the different TAD fabric designs (Fig. 7A) the same trends can be observed, but differences are much smaller, the corresponding penetrated air volumes (Fig. 7B) have no significant differences. The fabric designs are all of the same fabric specifications, with similar calipers and air permeabilities and yarn dimensions and weave structures. The focus in this comparison was to use fabrics with the closest possible behavior and see whether any differences could be achieved in outgoing solids while the air penetrating the structure was as similar as possible. The results in Fig. 7 show that this can be achieved, although nothing can be firmly concluded about the mechanisms behind the different outcomes. The TAD fabric 2 gives highest solids while fabric 4 gives lowest, they differ with approximately 1% at 20 ms vacuum dwell time. Scrutinizing the fabric parameters in Table 2, a low yarn density in CD and a high caliper seem to negatively affect solids content. Further investigations related to this need to be conducted for clear conclusions, but the method certainly allows this.

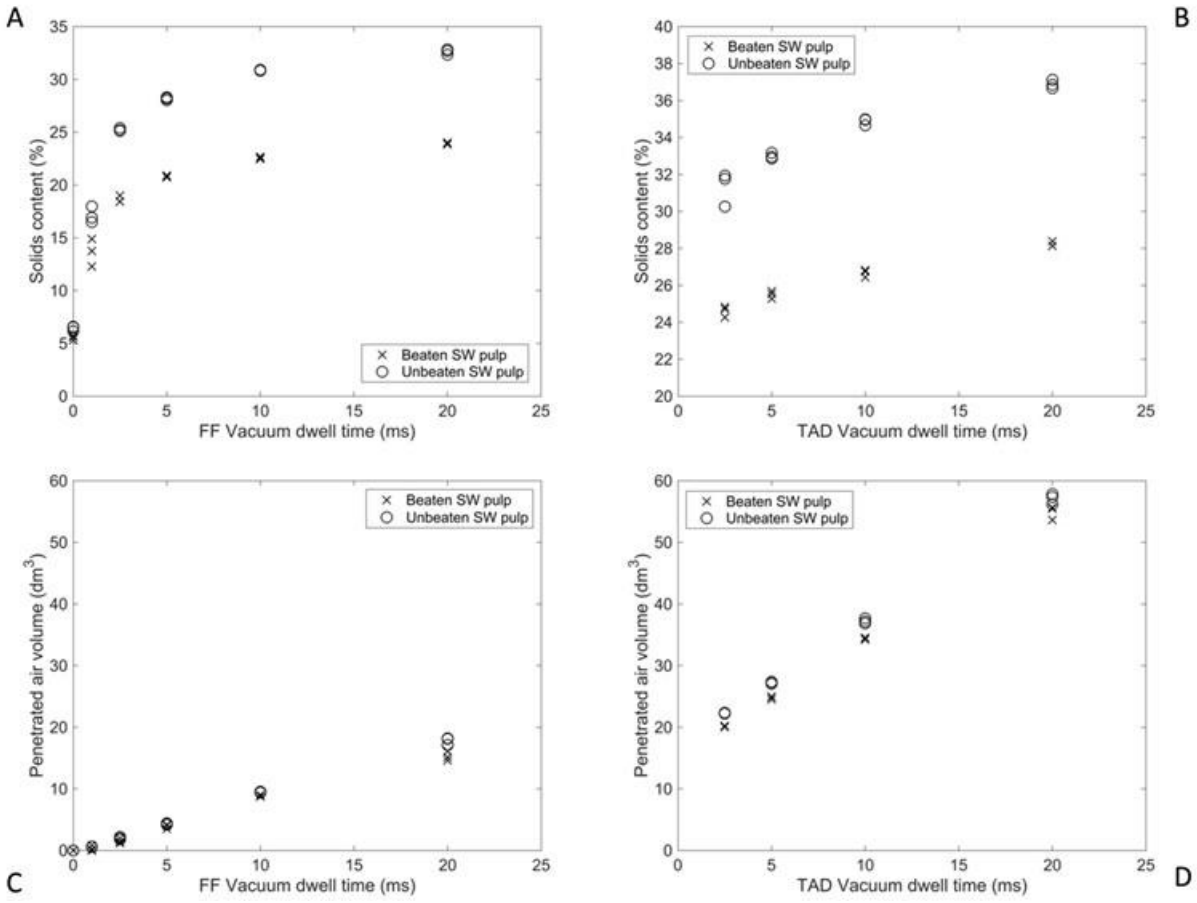

Fig. 6. Solids content (%) *versus* vacuum dwell time (ms) on the forming fabric (FF) (A), TAD fabric 1 (B), and penetrated air volume (dm^3) on the forming fabric (C) and TAD fabric 1 (D) in laboratory trials for the two beating levels. The fiber mix was 75/25 SW/HW and sheet basis weight 20 g/m^2

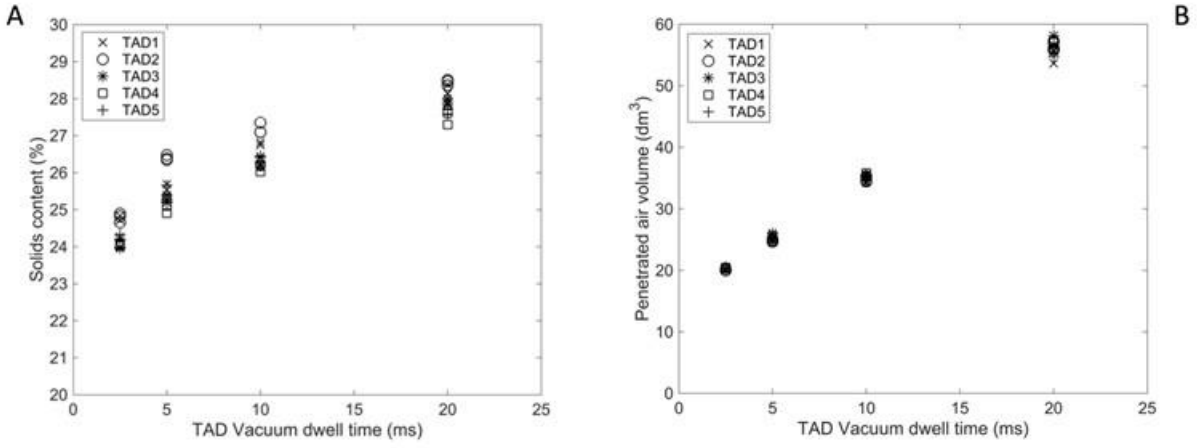

Fig. 7. Solids content (%) *versus* vacuum dwell time (ms) (A) and penetrated air volume (dm^3) (B) in laboratory trials for the five different TAD fabrics 1-5. The fiber mix was 75/25 SW/HW and sheet basis weight 20 g/m^2

Pilot Trial

The results from the solids content measurements from the pilot trial are shown in Table 10, which include the solids content positions before and after molding and after final Yankee drying. Measurement locations are indicated by arrows in Fig. 1. Pilot trial parameters are shown in Table 4.

Table 10. Solids Content Results from the Pilot Trial

Test	Solids Content (%) Before Molding	Solids Content (%) After Molding	Solids Content (%) After Yankee Drying
0	22.1 ± 0.1	26.5 ± 0.2	95.9 ± 0.7
1	21.5 ± 0.8	26.1 ± 0.1	97.3 ± 0.3
2	17.7 ± 0.6	22.1 ± 0.3	94.6 ± 0.7
3	25.1 ± 0.6	28.3 ± 0.1	98.2 ± 0.1
4	23.9 ± 0.1	27.6 ± 0.1	98.3 ± 0.2
5	19.9 ± 0.2	24.2 ± 0.1	97.5 ± 0.3
6	25.6 ± 0.4	28.8 ± 0.1	97.7 ± 0.6
7	16.8 ± 0.2	21.3 ± 0.1	94.6 ± 0.4
8	21.2 ± 0.3	25.4 ± 0.1	97.7 ± 0.3
9	22.6 ± 0.2	25.7 ± 0.1	96.9 ± 0.3
10	24.8 ± 0.1	25.7 ± 0.2	97.1 ± 0.6

Note: Mean values and 95% confidence intervals based on three repetitions; measurement locations: before and after molding, and after Yankee drying (indicated in Fig. 1)

Note that for test 0, the rush transfer remained by mistake at 0% (instead of 12%). This was not according to plan, and it impacted the sheet thickness. It was also observed a slight difference of 0.4% in solids content in between the conditions 0 and 1. Similarly, the tests 8 and 9 were performed at two distinct basis weights at the same rush transfer value. Results obtained in conditions 8 and 9 also indicated a minor difference in solids content (0.3%). This indicates that basis weight on the wire had no significant effect on the dry content achieved at molding box.

Despite of identical dry content results at the molding box for condition 8 and 9, the drying in the TAD section was found to be favorable to the higher basis weight condition due the higher resistance to the air flow. Greater area was available for the air to contact the fiber and migrating through the sheet. This improved the energy transferred from the air to the fiber and the water.

Results from the evaluation revealed a strong correlation of molding box solids content with the freeness at the headbox, as shown in Fig. 8. This is also supported by Fig. 9 showing a negative correlation in between geometric mean tensile and solids content, but to a lesser extent. The final paper's differences in moisture content may explain the poorer correlation.

The pilot evaluation confirmed a strong correlation between the dry content achieved out of the former and the result at the molding box (Fig. 10), which in turn also correlated well with the Canadian standard freeness (Fig. 8).

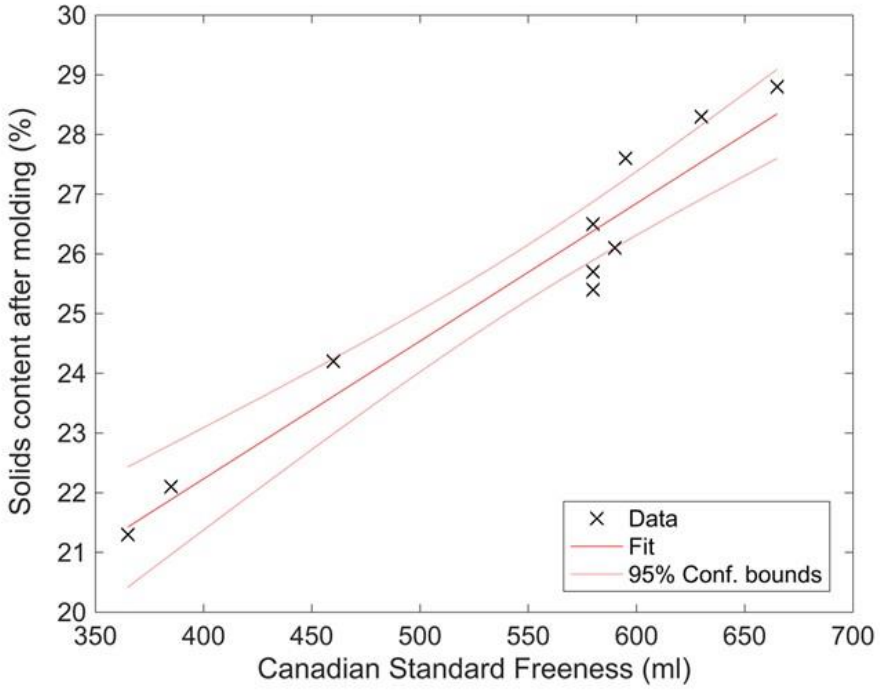

Fig. 8. Correlation between Canadian standard freeness (mL) and solids content after molding (%), including linear fit with 95% confidence boundaries. Data from pilot trials are shown in Table 10.

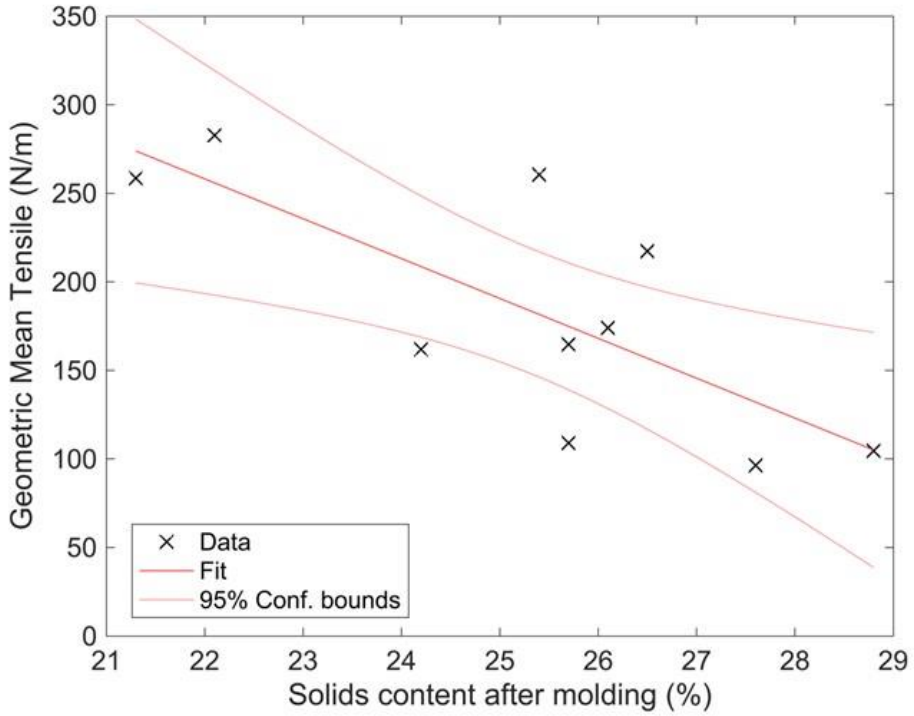

Fig. 9. Correlation between geometric mean tensile strength (N/m) and solids content after molding (%), including linear fit with 95% confidence boundaries. Data from pilot trials are shown in Table 10.

In condition 10, the vacuum was increased on the former for all dewatering boxes. While all other conditions were made with three consecutive vacuum dewatering boxes at -30, -40, -50 kPa, respectively, the vacuum on the former was raised to -50, -58, and -56 kPa for the test 10. Although the solids content on the former increased as a result of the vacuum change, the solids content out of the molding box remained unchanged. This data point deviated the most from the correlation shown by Fig. 10. Removing that data, the correlation factor increases substantially. This indicates that there is no point increasing the vacuum level too early in the process, which is well known in the literature (Hubbe *et al.* 2020; Sjöstrand 2023). The data correlations shown in Fig. 10 suggest that dry content out of the machine former could be used as a predictor for the solids content going to the TAD section if vacuum level is constant in the wet end.

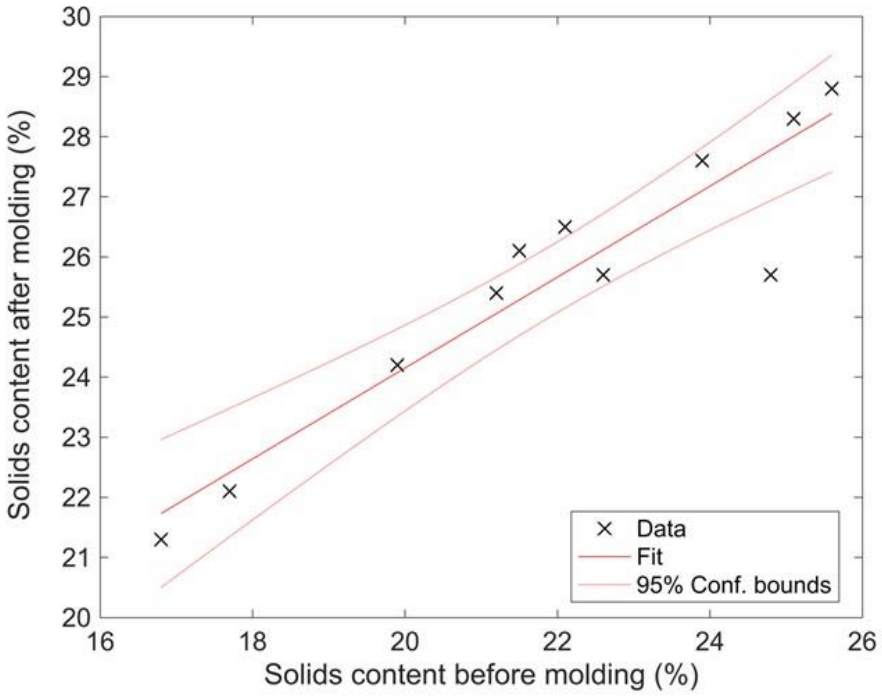

Fig. 10. Correlation between solids content before and after molding (%), including linear fit with 95% confidence boundaries. Data from pilot trials are shown in Table 10.

There will always be differences between laboratory scale and pilot or full scale when it comes to tissue manufacturing. Figure 11 shows the differences in sheet appearances for laboratory TAD and pilot TAD. It is evident that the molding with rush transfer into the TAD fabric of the pilot scale machine was not efficiently achieved at the laboratory scale. This conclusion is based on the bulkier structure of the pilot sheet (Fig. 11B) compared to the laboratory counterpart (Fig. 11A). This is also observed with the simpler measurement method of sheet caliper in Tables 5 through 9.

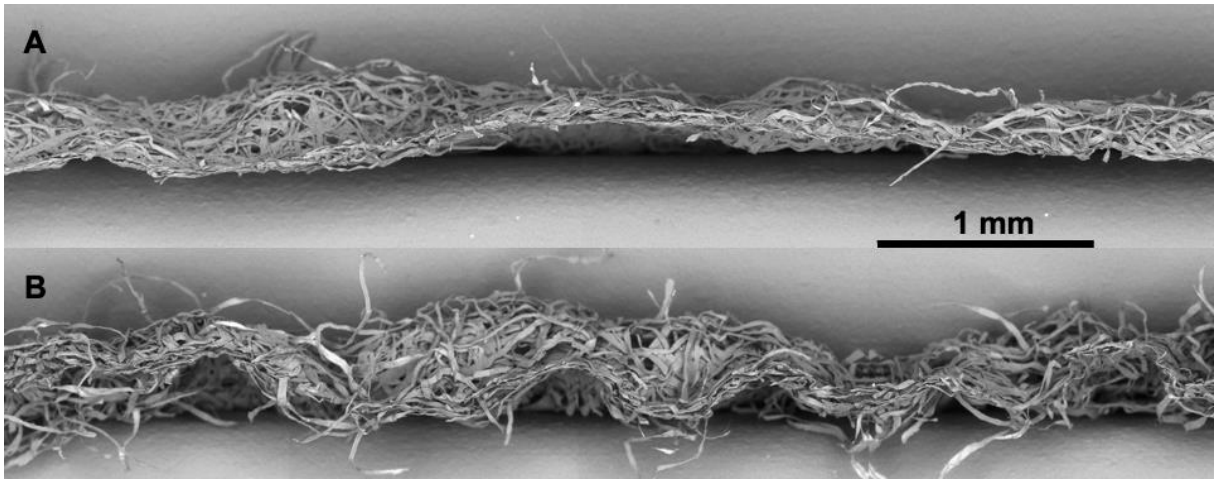

Fig. 11. SEM images of laboratory TAD sheet with 90/10 SW/HW fiber mix, beaten SW fibers, 20 g/m^2 basis weight and TAD fabric design 1 (A), and pilot TAD sheet from pilot run 6, which is the closest corresponding trials (B)

The laboratory solid contents result for forming fabric dewatering were compared with the pilot solids contents before molding, and the laboratory TAD dewatering were compared with pilot results after molding. In general, pilot solids were close to the corresponding laboratory solids. The values were slightly lower but still within the margin of error for the solids content measurements when exactly the same parameters were used. For example, solids content of laboratory forming fabric dewatering for 20, 25, and 30 g/m^2 (Fig. 4A) were around 24%, compared with solids before molding for pilot tests 9 and 10, 0 and 1, and 8, respectively, which ranged from 21.2% to 24.8%. The corresponding laboratory TAD dewatering solids (Fig. 4B) were 26 to 28%, and the pilot solids 25.4 to 26.5%. One important aspect is that the laboratory scale TAD occurs in another climate compared to pilot and full-scale TAD tissue production. The laboratory has a much lower temperature of approximately 20 °C and relatively dry air with low humidity. These results must therefore be evaluated carefully with this in mind.

The laboratory solids of different fiber mixes (Fig. 5A and 5B) were 24 to 26% on the forming fabric and 27 to 29% at the TAD, and for these the closest corresponding pilot tests 5, 2, and 7 showed solids contents of 21.3 to 24.2%, which is lower than laboratory values. Finally, the laboratory solids for beaten and unbeaten softwood pulps were 24 and 33% at the forming fabric and 28 and 37% at the TAD fabric, compared to pilot tests 3, 2 and 4, and 5, ranging between 17.7 to 25.1% before molding and 22.1 to 28.3% after molding, which is also considerably lower for pilot compared to laboratory values. It is important to note for all values with different beating levels that they are not exactly the same conditions for these measurements, mainly because the laboratory hardwood fibers were unbeaten, which can explain the higher solids contents with increasing percentages of those fibers in the fiber mix.

CONCLUSIONS

1. Mechanisms of dewatering during Through Air Drying (TAD) molding have previously been suggested as pure air displacement dewatering, whereas the new results from this work indicate that the mechanism rather is a combination of compression dewatering and air displacement dewatering.
2. The presence of rush transfer impact the visual sheet appearance, sheet thickness, and also slightly the achieved solids content.
3. There is a strong correlation of molding box solids content with the freeness at the headbox for TAD tissue manufacturing.
4. The pilot evaluation confirmed a strong correlation between the dry content achieved out of the former and the result at molding box.
5. The solids content out of the molding box correlated well with initial vacuum dewatering, drying energy could be saved by increasing efficiency in the early dewatering stages.
6. Solids contents of pilot trials correspond well to laboratory solids contents when identical conditions are used. This enables the described laboratory method to be used comprehensively to simulate pilot- and full-scale behavior of TAD tissue manufacturing.

ACKNOWLEDGMENTS

The authors are grateful for the financial support of the Knowledge foundation, Grant No. 2022-0024, as well as generous in-kind contributions from Albany International Inc., Karlstad University, and Valmet AB. Sara Christensson and Cecilia Westling at Stora Enso AB are gratefully acknowledged for providing beaten softwood pulp fibers. Jörgen Israelsson, Anders Ottosson, Karl-Johan Tolfsson, and Viktor Bergström at Valmet AB are acknowledged for help with ideas, consultations, and providing pilot scale data. Darrin Curley and John LaFond at Albany International Inc. are acknowledged for help with discussions regarding experiments and results. Magnus Lestelius and Carl-Anton Karlsson at Karlstad University are acknowledged for help with discussions and laboratory equipment.

REFERENCES CITED

Åslund, P., and Vomhoff, H. (2008a). "Method for studying the deformation of a fibre web," *Nordic Pulp & Paper Research Journal* 23(4), 398-402. DOI: 10.3183/npprj-2008-23-04-p398-402

Åslund, P., and Vomhoff, H. (2008b). "Dewatering mechanisms and their influence on suction box dewatering processes – A literature review," *Nordic Pulp & Paper Research Journal* 23(4), 389-397. DOI: 10.3183/npprj-2008-23-04-p389-397

ASTM D737-96 (2017). "Test method for air permeability of textiles," ASTM International, West Conshohocken, PA, USA.

Attwood, B. W. (1962). "A study of vacuum box operation," *Paper Technology* 3(5), 144-153.

Britt, K. W., and Unbehend, J. E. (1985). "Water removal during paper formation," *TAPPI Journal* 68(4), 104-107.

de Assis, T., Reisinger, L. W., Pal, L., Pawlak, J., Jameel, H., and Gonzalez, R. W. (2018). "Understanding the effect of machine technology and cellulosic fibers on tissue properties – A review," *BioResources* 13(2), 4593-4629. DOI: 10.15376/biores.13.2.Deassis

Holmberg, K., Siilasto, R., Laitinen, T., Andersson, P., and Jäsberg, A. (2013). "Global energy consumption due to friction in paper machines," *Tribology International* 62, 58-77. DOI: 10.1016/j.triboint.2013.02.003

Hubbe, M. A., Sjöstrand, B., Nilsson, N., Koponen, A., and McDonald, J. D. (2020). "Rate-limiting mechanisms of water removal during the formation, vacuum dewatering, and wet-pressing of paper webs: A review," *BioResources* 15(4), 9672-9755. DOI: 10.15376/biores.15.4.Hubbe

Håkansson, C. (2010). "Energy savings by process optimization. Reducing vacuum demand in the paper machine," in: *Proceedings of TAPPI PaperCon 2010*, Atlanta, GA, USA, pp. 1164-1191.

ISO 187 (2022). "Paper, board and pulps – Standard atmosphere for conditioning and testing and procedure for monitoring the atmosphere and conditioning of samples," International Organization for Standardization, Geneva, Switzerland.

ISO 638-1 (2022). "Paper, board, pulps and cellulosic nanomaterials – Determination of dry matter content by oven-drying method – Part 1: Materials in solid form," International Organization for Standardization, Geneva, Switzerland.

ISO 5267-1 (1999). "Pulps – Determination of drainability – Part 1: Schopper-Riegler method," International Standardization of Organization, Geneva, Switzerland.

ISO 12625-3 (2014). "Tissue paper and tissue products – Part 3: Determination of thickness, bulking thickness and apparent bulk density and bulk," International Organization for Standardization, Geneva, Switzerland.

Lahtinen, J., and Karvinen, J. (2010). "Energy savings in paper machine vacuum system. How to utilize modern process and variable speed drive technology," *Proceedings of TAPPI PaperCon 2010*, Atlanta, GA, USA, pp. 1129-1163.

Neun, J. A. (1994). "Performance of high vacuum dewatering elements in the forming section," *TAPPI Journal* 77(9), 133-138.

Neun, J. A. (1996). "High-vacuum dewatering of newsprint," *TAPPI Journal* 79(9), 153-157.

Nilsson, L. (2014a). "Stepwise development of a mathematical model for air flow in vacuum dewatering of paper," *Drying Technology* 32(13), 1587-1597. DOI: 10.1080/07373937.2014.909844

Nilsson, L. (2014b). "Air flow and compression work in vacuum dewatering of paper," *Drying Technology* 32(1), 39-46. DOI: 10.1080/07373937.2013.809732

Paulapuro, H. (2000). "Wet pressing," in: *Papermaking Part 1: Stock Preparation and Wet End*, H. Paulapuro, and J. Gullichsen (eds.), Fapet Oy, Jyväskylä, Finland, pp. 284-340.

Pujara, J., Siddiqui, M. A., Liu, Z., Bjegovic, P., Takagaki, S. S., Li, P. Y., and Ramaswamy, S. (2008). "Method to characterize the air flow and water removal characteristics during vacuum dewatering. Part II—Analysis and characterization," *Drying Technology* 26(3), 341-348. DOI: 10.1080/07373930801898125

Rahman, H., Engstrand, P., Sandström, P., and Sjöstrand, B. (2018). "Dewatering properties of low grammage handsheets of softwood kraft pulps modified to minimize the need for refining," *Nordic Pulp & Paper Research Journal* 33(3), 397-403. DOI: 10.1515/npprj-2018-3037

Räisänen, K. O., Karrila, S., and Maijala, A. (1996). "Vacuum dewatering optimization with different furnishes," *Paperi ja Puu* 78(8), 461-467.

Ramaswamy, S. (2003). "Vacuum dewatering during paper manufacturing," *Drying Technology* 21(4), 685-717. DOI: 10.1081/DRT-120019058

Sjöstrand, B. (2020). *Vacuum Dewatering of Cellulosic Materials*, Doctoral Thesis, Karlstad University, Karlstad, Sweden.

Sjöstrand, B. (2023). "Progression of vacuum level in successive vacuum suction boxes in a paper machine – Impact on dewatering efficiency and energy demand – A laboratory study," *BioResources* 18(2), 3642-3653. DOI: 10.15376/biores.18.2.3642-3653

Sjöstrand, B., Barbier, C., Ullsten, H., and Nilsson, L. (2019). "Dewatering of softwood kraft pulp with additives of microfibrillated cellulose and dialcohol cellulose," *BioResources* 14(3), 6370-6383. DOI: 10.15376/biores.14.3.6370-6383

Sjöstrand, B., Danielsson, M., and Lestelius, M. (2023). "Method for studying water removal and air penetration during through air drying of tissue in laboratory scale," *BioResources* 18(2), 3073-3088. DOI: 10.15376/biores.18.2.3073-3088

Sjöstrand, B., Barbier, C., and Nilsson, L. (2015). "Rewetting after high vacuum suction boxes in a pilot paper machine," *Nordic Pulp and Paper Research Journal*, *30*(4), 667–672. https://doi.org/https://doi.org/10.3183/npprj-2015-30-04-p667-672

Sjöstrand, B., Barbier, C., and Nilsson, L. (2016). "Influence on sheet dewatering by structural differences in forming fabrics," in: *Proceedings of TAPPI PaperCon 2016*, Cincinatti, OH, USA, pp. 767-776.

Sjöstrand, B., Barbier, C., and Nilsson, L. (2017). "Modeling the influence of forming fabric structure on vacuum box dewatering," *TAPPI Journal* 16(8), 477-483.

Sjöstrand, B., Barbier, C., Ullsten, H., and Nilsson, L. (2019). "Dewatering of softwood kraft pulp with additives of microfibrillated cellulose and dialcohol cellulose," *BioResources* 14(3), 6370-6383. DOI: 10.15376/biores.14.3.6370-6383

Sjöstrand, B., and Brolinson, A. (2022). "Addition of polyvinylamine in chemi-thermomechanical pulp and kraft pulp and the effects on dewatering, strength, and air permeance," *BioResources* 17(3), 4098-4115. DOI: 10.15376/biores.17.3.4098-4115

Stenström, S., and Nilsson, L. (2015). "Predicting water removal during vacuum dewatering from fundamental fibre property data," *Nordic Pulp & Paper Research Journal* 30(2), 265-271. DOI: 10.3183/npprj-2015-30-02-p265-271

Tysén, A. (2018). *Through Air Drying: Thermographic Studies of Drying Rates, Drying Non-uniformity and Infrared Assisted Drying*, Doctoral Thesis, Karlstad University, Karlstad, Sweden.

Tysén, A., Vomhoff, H., and Nilsson, L. (2015). "The influence of grammage and pulp type on through air drying," *Nordic Pulp & Paper Research Journal* 30(4), 651-659. DOI: 10.3183/npprj-2015-30-04-p651-659

Tysén, A., Vomhoff, H., and Nilsson, L. (2018). "Through air drying assisted by infrared radiation: The influence of radiator power on drying rates and temperature," *Nordic Pulp & Paper Research Journal* 33(4), 581-591. DOI: 10.1515/npprj-2018-2002

Vieira, J. C., Fiadeiro, P. T., and Costa, A. P. (2023). "Converting operations impact on tissue paper product properties – A review," *BioResources* 18(1), 2303–2326. DOI: 10.15376/biores.18.1.Vieira

Article submitted: September 13, 2023; Peer review completed: October 14, 2023; Revised version received and accepted: October 16, 2023; Published: October 19, 2023.
DOI: 10.15376/biores.18.4.8264-8283